

This article was downloaded by:

On: 28 January 2011

Access details: *Access Details: Free Access*

Publisher *Taylor & Francis*

Informa Ltd Registered in England and Wales Registered Number: 1072954 Registered office: Mortimer House, 37-41 Mortimer Street, London W1T 3JH, UK



Physics and Chemistry of Liquids

Publication details, including instructions for authors and subscription information:

<http://www.informaworld.com/smpp/title~content=t713646857>

Direct Correlation Function Properties of Liquid Metals Near Freezing

J. M. Bernasconi^a; N. H. March^a

^a Theoretical Chemistry Department, University of Oxford, Oxford, England

To cite this Article Bernasconi, J. M. and March, N. H. (1986) 'Direct Correlation Function Properties of Liquid Metals Near Freezing', *Physics and Chemistry of Liquids*, 15: 3, 169 – 183

To link to this Article: DOI: 10.1080/00319108608078479

URL: <http://dx.doi.org/10.1080/00319108608078479>

PLEASE SCROLL DOWN FOR ARTICLE

Full terms and conditions of use: <http://www.informaworld.com/terms-and-conditions-of-access.pdf>

This article may be used for research, teaching and private study purposes. Any substantial or systematic reproduction, re-distribution, re-selling, loan or sub-licensing, systematic supply or distribution in any form to anyone is expressly forbidden.

The publisher does not give any warranty express or implied or make any representation that the contents will be complete or accurate or up to date. The accuracy of any instructions, formulae and drug doses should be independently verified with primary sources. The publisher shall not be liable for any loss, actions, claims, proceedings, demand or costs or damages whatsoever or howsoever caused arising directly or indirectly in connection with or arising out of the use of this material.

Direct Correlation Function Properties of Liquid Metals Near Freezing

J. M. BERNASCONI and N. H. MARCH

*Theoretical Chemistry Department, University of Oxford, 1 South Parks Rd.,
Oxford OX1 3TG, England*

(Received July 2, 1985)

Motivated by the prediction of the Percus–Yevick hard sphere solution that, for dense liquids, the ratio $R = c(r=0)/\tilde{c}(q=0)$ is very near to unity, $c(r)$ being the direct correlation function and $\tilde{c}(q)$ its Fourier transform, this ratio has been calculated from diffraction plus thermodynamic data for some fifteen liquid metals near their freezing points. It is found that $0.2 < R < 1.3$, but for the liquid alkalis, the noble metals and the first row transition metals chosen, R is near to unity. This is to be contrasted with $R \sim 2$ for liquid argon near the triple point.

The polyvalent metals Ga, Pb and Sn, with the smallest values of R , are plainly totally at variance with the hard sphere prediction. However, R is near to unity for Na, K and Rb and yet it is known from neutron inelastic scattering that Rb exhibits a collective mode and is therefore quite different from a hard sphere liquid also. In fact, by examining long-range damping in $\tilde{c}(q)$ for Na and Pb, we conclude that Pb has the harder core of these two metals.

Finally it is argued that for Pb, $c(r)$ remains negative and non-zero just outside the “core” diameter and this then accounts immediately for the low value of R , as also in the cases of Ga and Sn. In contrast, for argon $c(r)$ has passed through a node before or at the core diameter, leading to R much greater than unity.

1 INTRODUCTION

In structural theories of liquids, the direct or Ornstein–Zernike correlation function $c(r)$ continues to play an important role. This function is related to the pair distribution function $g(r)$ of the liquid through the defining equation

$$h(r) = c(r) + \rho \int c(|\mathbf{r} - \mathbf{r}'|)h(r') \, d\mathbf{r}' \quad (1.1)$$

where the total correlation function $h(r)$ is simply $g(r) - 1$, while ρ is the atomic number density.

As an example, for a simple monatomic liquid like argon, a reasonable approximation to $c(r)$ was given in the work of Woodhead-Galloway *et al.*¹ as

$$c(r) = c_{\text{hard sphere}}(r) - \frac{\phi_{\text{long range}}(r)}{k_B T} \quad (1.2)$$

where $\phi_{\text{long-range}}(r)$ is equivalent to the assumed pair potential $\phi(r)$ outside the hard core of diameter σ . Using the Percus-Yevick solution^{2,3} for $c_{\text{hard sphere}}(r) \equiv c_{\text{hs}}(r)$ and noting that this is identically zero outside $r = \sigma$ in this approximate theory, it is evident from Eq. (1.2) that

$$c(r) \simeq -\frac{\phi(r)}{k_B T}, \quad r > \sigma. \quad (1.3)$$

However, we presently know of no decisive evidence that Eq. (1.3) is true for liquid metals, on which we focus attention in the present paper.

Bhatia and March⁴ noted that, in the case of the Percus-Yevick solution for hard spheres

$$\tilde{c}_{\text{hs}}^{\text{PY}}(0) = 1 + c_{\text{hs}}(r = 0) \quad (1.4)$$

where $\tilde{c}(q)$ is the Fourier transform of $c(r)$ defined through

$$c(r) = \frac{1}{8\pi^3\rho} \int_0^\infty \tilde{c}(q) \frac{\sin qr}{qr} 4\pi q^2 dq \quad (1.5)$$

or in terms of the liquid structure factor $S(q)$:

$$\tilde{c}(q) = \frac{S(q) - 1}{S(q)}. \quad (1.6)$$

Now the hard-sphere Percus-Yevick solution yields

$$c_{\text{hs}}(r = 0) \simeq -(1 + 2\eta)^2 / (1 - \eta)^4 \quad (1.7)$$

where η is the packing fraction $(\pi/6)\rho\sigma^3$. For many simple liquids near the melting temperature, $\eta \simeq 0.45$ and inserting this into Eq. (1.7) yields a value of ~ -40 .

Although, as we shall confirm below, this is a reasonable estimate of $c(r = 0)$ for liquid argon, the experimental value being -33 , the relation to $\tilde{c}(q = 0)$ given in Eq. (1.4) for hard spheres fails. This implies that the

attractive tail $\phi_{\text{long range}}(r)$ makes an important contribution to $\tilde{c}(q = 0)$. In fact, whereas Eq. (1.4) yields the ratio

$$R = \frac{c(r = 0)}{\tilde{c}(q = 0)} \quad (1.8)$$

to be approximately unity from the Percus-Yevick hard sphere solution, as $|c(r = 0)| \gg 1$ for argon near the melting temperature, we find in practice that $R \sim 2$.

Turning from liquid argon to liquid metals, we find, to us somewhat surprisingly, that the hard-sphere value of $c(r = 0)$ turns out to be a reasonable one for metals also. Though experimental errors are quite substantial, $-c(r = 0)$ turns out to fall in the range 34–50, with the exception of Cu at a value of 60, to be compared with the value of 40 for hard spheres.

However, $-\tilde{c}(q = 0)$ varies more widely, as expected from the above discussion of argon, and for the liquid metals considered in the present work, the range is from ~ 40 –200. In this paper, though we utilize liquid argon for purposes of comparison, the major interest is in a variety of liquid metals.

2 CALCULATION OF $R = c(r = 0)/\tilde{c}(q = 0)$ FOR LIQUID METALS FROM EXPERIMENT

Values of $c(r = 0)$ for liquid metals near their freezing points have been calculated from experimental diffraction data for $S(q)$, and these results are recorded in Table I. $\tilde{c}(q = 0)$ obtained from experimental data on the isothermal compressibility is also recorded there. The final column of Table I gives the ratio R defined in Eq. (1.8).

Errors in $-c(r = 0)$, $-\tilde{c}(q = 0)$ and hence R have been estimated by using different sets of experimental data. This demonstrates that errors in R can be substantial; at times as great as ± 0.2 . On this basis alone, therefore, one would find it difficult to distinguish the results of some nine of the fifteen metals in Table I from the hard sphere prediction $R = 1$. However, though we shall discuss the problem of obtaining reliable data for R a little further immediately below, there can be no doubt that the liquid metals Ga, Pb and Sn have $R \ll 1$, and that, as already discussed, the case of argon included in Table I for purposes of comparison with the metals, has R substantially greater than unity.

The problem of obtaining reliable data can be seen by considering what region of the structure factor $S(q)$ dominates the value of $c(r = 0)$. From Eq. (1.5), when $r = 0$ one has

$$c(r = 0) = \frac{1}{8\pi^3\rho} \int_0^\infty 4\pi\tilde{c}(q)q^2 dq. \quad (2.1)$$

Even allowing for the factor q^2 in the integrand of Eq. (2.1), it turns out that, since $\tilde{c}(q)$ is large and negative at small q , the integral in Eq. (2.1) is dominated by the region of q well inside the first peak of $S(q)$ (cf. Appendix A1 also). It is this relatively small angle scattering region which is still the least well studied region of the structure factor in liquid metals to date.

Though we shall return to a discussion of why R is very small in Ga, Pb and Sn below, we can see why, from the available data, R is low in these metals. As is demonstrated in Appendix A2, a localized form of $\tilde{c}(q)/\tilde{c}(0)$, which in turn suggests a long-range pair potential, results in a low value of the ratio R .

From the standpoint of the data for this ratio alone, as recorded in Table I, it might seem tempting to conclude that the liquid alkali metals Na, K and Rb are hard-sphere liquids. However, it is well known for liquid Rb from the neutron inelastic scattering studies of Copley and Rowe¹⁶ that a well defined collective mode exists for this metal; a feature which is, of course, totally foreign to any hard-sphere liquid. Hence it is already plain that R near to unity is a necessary but not a sufficient condition to conclude that a liquid metal is hard-sphere like.

TABLE I

Ratio : direct correlation function $c(r)$ at $r = 0$ divided by $\tilde{c}(q)$, its Fourier transform, evaluated at $q = 0$, near melting temperature.

Liquid metal	$-c(r = 0)$	$-\tilde{c}(q = 0)$	$R = c(r = 0)/\tilde{c}(q = 0)$
Na ^{5,6,7}	43	41	1.0
K ^{5,6,7}	42	40	1.0
Rb ⁶	45	42	1.1
Cs ^{6,7}	50	38	1.3
Cu ^{8,9}	60	47	1.3
Ag ⁹	51	53	1.0
Au ⁹	35	38	0.9
Mg ^{6,10}	31	39	0.8
Al ^{6,11}	45	54	0.8
Ga ¹²	34	200	0.2
Pb ¹²	44	110	0.4
Sn ^{10,13}	40	140	0.3
Fe ⁹	46	48	1.0
Ni ^{9,14}	41	50	0.8
Co ⁹	35	50	0.7

For comparison, we note that for liquid argon the values are

$$-c(r = 0) = 33, \quad -\tilde{c}(q = 0) = 17 \quad \text{and} \quad R \sim 2.$$

3 USE OF SIMPLE COLLECTIVE MODE MODEL FOR LIQUID Rb

To press the above point, let us consider briefly in this section the prediction of a simple collective mode model for Rb. The arguments underlying this model can be traced back to Feynman's work on the Bose liquid ^4He at absolute zero. One constructs a dynamical structure factor $S(q, \omega)$, which when integrated over all frequencies yields the static structure factor $S(q)$ and which satisfies, for a classical liquid

$$\int_{-\infty}^{\infty} S(q, \omega) \omega^2 d\omega = \frac{k_B T q^2}{M} \quad (3.1)$$

where M is the ionic mass.

Following Feynman, one assumes that the collective mode, with dispersion $\omega(q)$, exhausts the sum rule (3.1), i.e. one inserts into Eq. (3.1) the ansatz

$$S(q, \omega) = \frac{1}{2} S(q) [\delta(\omega - \omega(q)) + \delta(\omega + \omega(q))] \quad (3.2)$$

to obtain the relation between structure factor and collective mode dispersion relation $\omega(q)$:

$$\omega^2(q) = \frac{k_B T q^2}{M S(q)} = \frac{k_B T q^2 (1 - \tilde{c}(q))}{M} \quad (3.3)$$

In the limit q tends to zero, $\omega(q) \rightarrow v_s q$, where v_s is the velocity of sound, whereas the right-hand side of Eq. (3.3), when one uses the result of fluctuation theory that

$$S(0) = \rho k_B T K_T = \frac{\gamma k_B T}{M v_s^2} \quad (3.4)$$

with K_T the isothermal compressibility and γ the ratio of the specific heats c_p/c_v , yields this same value only if γ is equal to unity. In practice, this is not serious since γ is around 1.2 to 1.3 for many liquid metals near freezing, so that the formula (3.3) is useful at least in the long wavelength limit in such cases.

This is the point at which we should note that a collective mode has been observed in Pb^{17} as well as in Rb, and an approximate calculation of the ratio R from the measured dispersion curves $\omega(q)$ for these two metals can yield some further insight into the problem. In Figure 3.1 the measured dispersion curves of the two liquid metals are reproduced. The point we want to stress here is that Pb is more dispersive than Rb in that departures from the long wavelength, or small q , limit $\omega(q) = v_s q$ occur more quickly for Pb than for Rb. The effect of this on the calculated value for $\tilde{c}(q)$ according to Eq. (3.3) is to produce a more localized $\tilde{c}(q)$ for Pb than for Rb, which reduces the ratio R as already noted (see also Appendix A, Section A2).

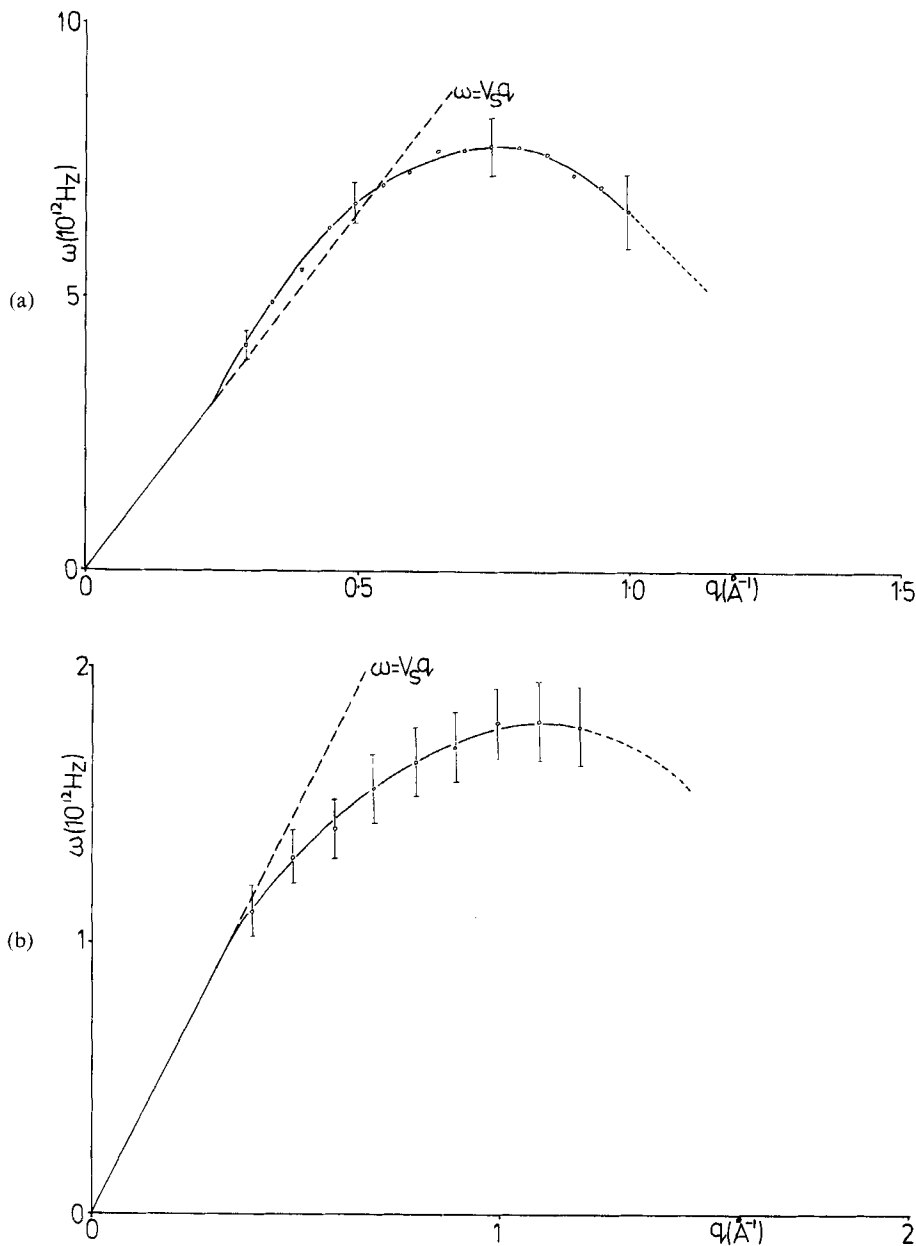


FIGURE 3.1 Collective mode dispersion curves extracted from neutron inelastic experiments on (a) Rb and (b) Pb.

The long wavelength limiting form $\omega(q) = v_s q$, with v_s the velocity of sound in the liquid metal is also shown. What is important in the present context is that Pb departs earlier from the long wavelength limiting behaviour than does Rb. From Eqn. (3.3), this in turn implies that $\tilde{c}(q)$ is more localized at small q for Pb than for Rb.

We should caution, however, that the above arguments are meant only to provide some additional insight into the differences between Pb and Rb; they are not quantitatively valid as Eq. (3.3), taken quite literally, would overestimate by about a factor of 2 the values of $|c(r = 0)|$.

4 VALUE OF R AND ITS CONSEQUENCE FOR THE DIRECT CORRELATION FUNCTION $c(r)$

We turn now to examine specifically the three liquid metals in Table I which, beyond reasonable doubt, in spite of large experimental errors, have the ratio R very different from, and all less than, unity.

To see how such a situation can arise, we return to Eq. (1.1) and put $r = 0$. Since, for a classical liquid, we know that $g(r = 0) = 0$, and hence $h(r = 0) = -1$, we find

$$-1 = c(r = 0) + \rho \int c(r') [g(r') - 1] dr'. \quad (4.1)$$

But $\rho \int c(r') dr' = \tilde{c}(q = 0)$ and hence

$$\tilde{c}(q = 0) = 1 + c(r = 0) + \rho \int g(r)c(r) dr. \quad (4.2)$$

This Eq. (4.2) is the formally exact generalization of the Percus–Yevick hard sphere result (1.4). This latter result follows, almost trivially, from Eq. (4.2), when we note that for hard spheres $g(r) = 0$ inside the hard core diameter, whereas $c_{hs}^{PY}(r) = 0$ outside σ , and hence the integral in Eq. (4.2) is identically zero for this case.

Rearranging Eq. (4.2), we can write for the ratio R in Eq. (1.8):

$$R = 1 - \frac{1}{\tilde{c}(q = 0)} - \frac{\rho}{\tilde{c}(q = 0)} \int g(r)c(r) dr. \quad (4.3)$$

Plainly, by inspection of Table I, the term $1/\tilde{c}(q = 0)$ is small, and appreciable deviation of R from unity must be sought in the final term in Eq. (4.3). Hence, we will concentrate on this term for the three liquid metals with very small R and also, for purposes of comparison, for argon with $R \sim 2$.

Since in real liquids, $g(r)$ is still practically zero inside a core diameter, and since $\tilde{c}(q = 0)$ is negative near freezing, R can only be appreciably less than unity from Eq. (4.3) if $c(r)$ has a negative region of appreciable amplitude outside the diameter σ . Conversely, R for Ar can only be appreciably greater than unity if $c(r)$ has already become positive either at, or inside, the hard core diameter. This is schematically depicted in Figure 4.1. While a node in

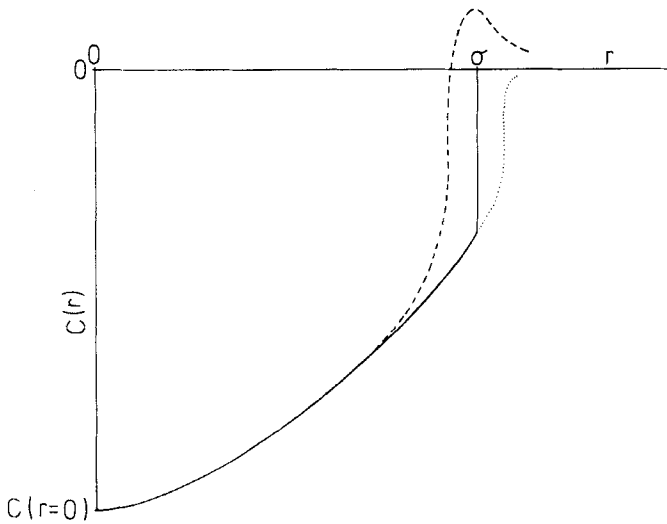


FIGURE 4.1 Schematic forms of direct correlation function $c(r)$.

Solid curve depicts the Percus–Yevick hard sphere form.

Dashed curve is schematic form for liquid argon near triple point.

Dotted curve is schematic form for liquid Pb, Sn and Ga.

Note that for argon the node in $c(r)$ is at, or inside, the hard core diameter σ . In contrast, for liquid Pb, Sn and Ga, $c(r)$ has a negative region of significant magnitude outside the hard core diameter. The precise form of $c(r)$ outside σ is not presently known for these three metals, either from theory or experiment.

$c(r)$ is an important structural feature for liquid argon, we know of no definitive proof, either from theory or experiment for liquid metals, that one or more nodes exist in $c(r)$. However, provided Eq. (1.3) again comes into its own at sufficiently large r , the oscillatory behaviour of potentials in liquid metals would imply a succession of nodes in $c(r)$ at sufficiently large distances.

5 CORE HARDNESS AND LONG-RANGE OSCILLATIONS IN $\tilde{c}(q)$

It is known from general Fourier transform theory that a sharp edge in r space at non-zero r will lead to long-range oscillations in q space. Thus, the Percus–Yevick $c(r)$ for hard spheres, with a marked discontinuity at σ as depicted in Figure 4.1, will lead to pronounced long-range oscillations in $\tilde{c}(q)$. All real liquids will be softer than this, and one can compare the damping of the long-range oscillations as observed in diffraction experiments with the hard sphere results.

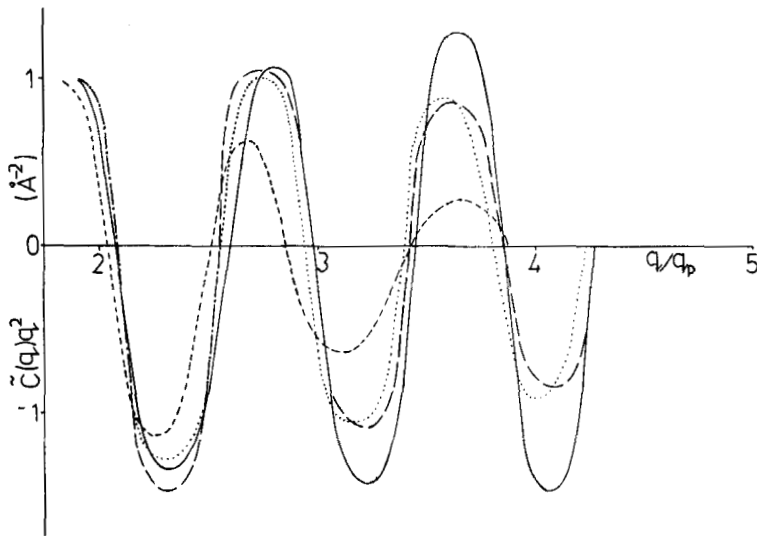


FIGURE 5.1 Shows large q oscillations in the quantity $q^2\tilde{c}(q)$, with $\tilde{c}(q)$ the Fourier transform of $c(r)$.

Hard spheres	—————
Argon	- - - - -
Na	- · - · - ·
Pb	· · · · ·

In the Figure, the independent variable is the reduced wave number q/q_p where q_p is the position of the first peak in the structure factor $S(q)$. The first peak shown in the Figure is actually the second peak occurring in $q^2\tilde{c}(q)$ and these first peaks are all scaled to unity for purposes of comparison.

The damping of the successive peaks in $q^2\tilde{c}(q)$ can be represented approximately by a factor $\exp(-\alpha q)$. Table II indicates that α is substantially less for Pb and Ar than for Na. This means that Pb and Ar must exhibit a more abrupt rise in $c(r)$ near the hard core diameter than Na; i.e. Pb and Ar are "harder" core liquids than Na.

The detailed way in which this has been done is outlined in Appendix B, Eq. (B4). However, Figure 5.1 shows $q^2\tilde{c}(q)$ versus q for Ar, Na and Pb, compared with a suitable hard sphere curve. Representing the damping of the peaks in $q^2\tilde{c}(q)$ by a factor $\exp(-\alpha q)$, where α measures how abruptly $c(r)$ rises around the core diameter σ , the values of α thereby deduced, discussed in a little detail in Appendix B, are recorded in Table II. Of the three liquids whose long-range behaviour is depicted in Figure 5.1, it is clear that $c(r)$ rises abruptly near σ in both Pb and Ar despite the fact that $R \ll 1$ for Pb and $R \gg 1$ for Ar.

To check that the low values of both α and R can be reconciled for Pb, we

have shown that only a relatively minor softening of the edge in the Percus–Yevick hard sphere form of $c(r)$ is required to reduce R to a low value. The modelling of liquid Pb was based on the hard sphere $c^{\text{PY}}(r)$, plus a term added from $r = \sigma$ to infinity, namely

$$c(r) = c^{\text{PY}}(r), r < \sigma$$

$$= \frac{\sigma c(\sigma)}{r} \exp\left\{-\lambda\left(\frac{r}{\sigma} - 1\right)\right\}, r > \sigma.$$

The parameter λ was used to fit the transform of the above function at $q = 0$ to the experimental value of $\tilde{c}(q = 0)$ and hence R , for Pb. The value $\lambda = 1.2$ gives the required ratio $R \sim 0.4$. This fairly large value of λ ensures a rapidly decreasing function for $r > \sigma$ and hence only a slight softening of the hard sphere edge in $c(r)$. This demonstrates that $\tilde{c}(q = 0)$ and hence R is sensitive to the region of $c(r)$ around $r = \sigma$. It must be cautioned, however, that the above model loses the first peak in $S(q)$, and hence also demonstrates the sensitivity of this peak to the precise form of $c(r)$ around $r = \sigma$.

6 CONCLUSION AND SUMMARY

For a whole set of liquid metals near freezing, there are clear departures from the Percus–Yevick hard sphere prediction $R \simeq 1$ only for Ga, Pb and Sn. However, it has also been clearly demonstrated that $R \simeq 1$ is far from a sufficient condition for a real liquid to be hard sphere-like. Indeed, R is near to unity for Rb, but Ga, Pb and Sn as well as the liquid insulator Ar, all of which have harder cores than Rb, show large departures from $R = 1$.

To gain further insight into the behaviour of the simpler metals, we have explored the consequences of a simple collective mode model for both Rb and Pb, in which metals neutron inelastic scattering experiments have demonstrated the presence of such collective modes. The smaller value of R is shown to occur in the metal where the greater collective mode dispersion is observed.

In argon, an important structural feature of $c(r)$ is the node around the hard core diameter. The fact that this node occurs either at, or slightly before, the hard core diameter, is shown to be responsible for the large value of the ratio R . No liquid metal of the fifteen examined in this work resembles this, R being less than 1.3 for them all. For the three metals Ga, Sn and Pb with really small values of R , the rise in $c(r)$ to zero at or below the core diameter in Ar is replaced by a form of $c(r)$ with a substantial negative region outside the core.

It would be of considerable interest in these three metals Ga, Pb and Sn if further and more precise diffraction studies could map out $c(r)$ accurately

outside the hard core. This seems to be an essential prerequisite to attempts to extract a potential for liquid metals from experimental structure data, along lines proposed by Johnson and March^{18,19} and applied very recently with considerable success²⁰ to the structure factor $S(q)$ obtained from computer simulation of liquid Al.

References

1. J. Woodhead-Galloway, T. Gaskell and N. H. March, *J. Phys.*, **C1**, 271 (1968).
2. M. S. Wertheim, *Phys. Rev. Lett.*, **10**, 321 (1963).
3. E. Thiele, *J. Chem. Phys.*, **39**, 474 (1963).
4. A. B. Bhatia and N. H. March, *J. Chem. Phys.*, **80**, 2076 (1984).
5. A. J. Greenfield, J. Wellendorf and N. Wiser, *Phys. Rev.*, **A4**, 1607 (1971).
6. Y. Waseda, *Z. Naturforsch.*, **38a**, 509 (1983).
7. M. J. Huijben and W. van der Lugt, *Acta Cryst.*, **A35**, 431 (1979).
8. M. Breuil and G. Tourand, *J. Phys. Chem. Solids*, **31**, 549 (1970).
9. Y. Waseda and M. Ohtani, *Phys. Stat. Sol B*, **62**, No 2, 535 (1974).
10. R. Kumaravadivel and R. Evans, *J. Phys.*, **C9**, 3877 (1976).
11. *Inst. Phys. Conf. Ser. No. 30*, p. 120 (Bristol) (1977).
12. C. A. Croxton, *Liquid State Physics*, Cambridge: University Press (1974).
13. D. Jovic and I. Padureanu, *J. Phys.*, **C9**, 1135 (1976).
14. Y. Waseda, K. Suzuki, S. Tamaki and S. Takeuchi, *Phys. Stat. Sol.*, **39**, 18 (1970).
15. J. L. Yarnell, M. J. Katz, R. G. Wenzel and S. H. Koenig, *Phys. Rev.*, **A7**, 2130 (1973).
16. J. R. D. Copley and J. M. Rowe, *Phys. Rev. Lett.*, **32**, 52 (1974).
17. O. Söderström, J. R. D. Copley, J. B. Suck and B. Dorner, *J. Phys.*, **F10**, L151 (1980).
18. M. D. Johnson and N. H. March, *Phys. Lett.*, **3**, 313 (1963); see also G. K. Corless and N. H. March, *Phil. Mag.*, **6**, 1285 (1961).
19. M. D. Johnson, P. Hutchinson and N. H. March, *Proc. Roy. Soc.*, **A282**, 283 (1964).
20. D. Levesque, J. J. Weis and L. Reatto, *Phys. Rev. Lett.*, **54**, 451 (1985).

Appendix A Schematic representation and modelling of the direct correlation function

We collect together here some schematic forms of properties of $c(r)$ and its Fourier transform $\tilde{c}(q)$ that we have used in the main text, together with some of the models we have found useful. We divide the Appendix, for convenience, into two short sections.

A1 SCHEMATIC FORMS OF $S(q)$, $\tilde{c}(q)$ AND $q^2\tilde{c}(q)$

For all the cases we have treated, the schematic forms of $S(q)$, $\tilde{c}(q)$ and $q^2\tilde{c}(q)$ are as shown in Figure A1. Part (a) is the same schematic form of $S(q)$ for all monatomic liquids; whether metals or insulators such as liquid

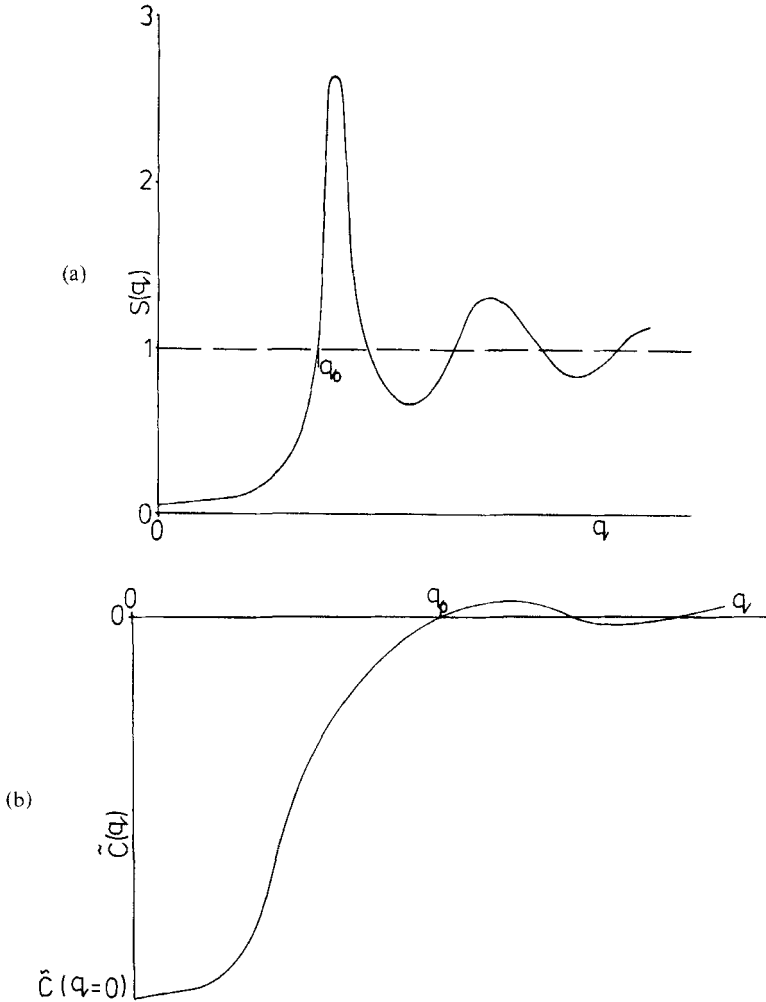


FIGURE A1 Schematic forms of: (a) Structure factor $S(q)$ versus q ; (b) Fourier transform $\tilde{c}(q)$ of direct correlation function $c(r)$ versus q . (c) $q^2\tilde{c}(q)$ versus q .

Main point to be noted here is that the area under the $q^2\tilde{c}(q)$ curve, which in turn determines $c(r=0)$, is dominated by the region well inside the first peak of the structure factor $S(q)$, that is by $q < q_0$, this latter quantity denoting the position of the first node in $\tilde{c}(q)$.

argon. The height of the first peak in $S(q)$ is known to be around 2.8 for most monatomic liquids just above their freezing points, a condition fulfilled by all the data employed in the present paper. The shape of $\tilde{c}(q)$ in Figure A1(b) follows then from $\tilde{c}(q) = 1 - S(q)^{-1}$. The calculation of $c(r=0)$, recorded for fifteen metals in Table I, involves from Eq. (2.1) the

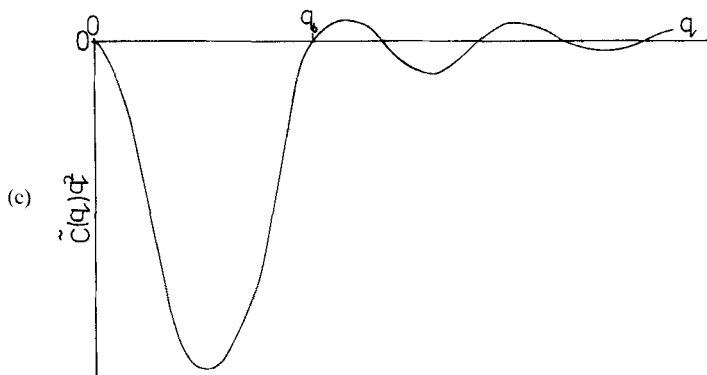


FIGURE A1 (continued)

integrand $q^2 \tilde{c}(q)$ which is therefore shown schematically in Figure A1(c). The important point to note about this integrand is that, when used to evaluate $c(r=0)$ in Eq. (2.1), the area between $q=0$ and $q=q_0$, the value of q at which $S(q)$ is first equal to unity, contributes at least 90% of the total area. The oscillations in $\tilde{c}(q)$ are quite small and their contributions tend to cancel.

A2 SCHEMATIC FORM OF $\tilde{c}(q)/\tilde{c}(q=0)$

The experimentally known forms of $\tilde{c}(q)/\tilde{c}(q=0)$ are contrasted for Ar, for which $R \sim 2$, and Pb, with $R \sim 0.4$, in Figure A2. We find that a localized form of $\tilde{c}(q)/\tilde{c}(q=0)$ leads to a low value of R , as follows from the fact that in Eq. (2.1) we must weight $\tilde{c}(q)$ by q^2 to calculate $c(r=0)$. Such localization in q space also suggests a long-range pair potential.

Appendix B Modelling of core hardness through damping of oscillations in hard sphere form of $\tilde{c}(q)$

Using the Percus–Yevick hard sphere form of the direct correlation function $c(r)$, namely

$$c^{\text{PY}}(r) = a_0 + a_1 \left(\frac{r}{\sigma} \right) + a_3 \left(\frac{r}{\sigma} \right)^3, \quad r < \sigma \quad (\text{B1})$$

$$= 0, \quad r > \sigma$$

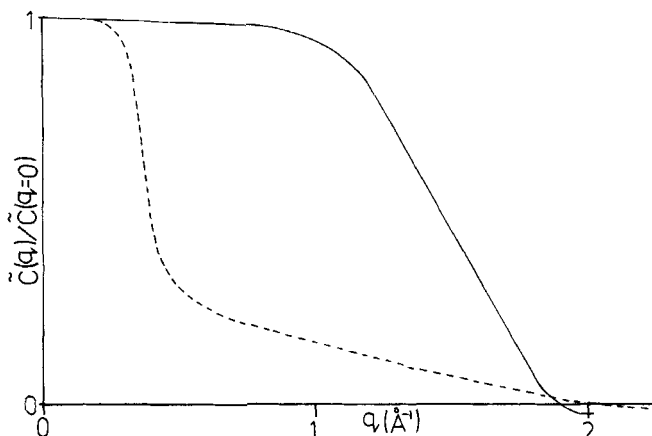


FIGURE A2 Contrasts forms of $\tilde{c}(q)/\tilde{c}(q=0)$ for argon (solid curve) and lead (dashed curve).¹²

and the transform relation

$$\tilde{c}(q) = \rho \int_0^{\infty} c(r) \frac{\sin qr}{qr} 4\pi r^2 dr, \quad (\text{B2})$$

the form of $\tilde{c}(q)$ for sufficiently large q turns out to be

$$\tilde{c}^{\text{PY}}(q) = K \frac{\cos q\sigma}{q^2}, \text{ as } q \text{ tends to infinity.} \quad (\text{B3})$$

Thus for hard spheres one would expect that $q^2c(q)$ would be relatively undamped at large q . This is borne out in Figure 5.1, even though in the hard sphere curve there we have made use of computer simulation results.¹²

Therefore, we shall attempt to model the real $\tilde{c}(q)$ for the liquids Ar, Na and Pb, at large q , by a damped version of the hard sphere $c(q)$:

$$\tilde{c}(q) = \tilde{c}_{\text{hs}}(q) \exp(-\alpha q). \quad (\text{B4})$$

Then we have calculated the value of α , by first scaling the second peak to unity, as in Figure 5.1, and writing

$$\ln \frac{q^2 \tilde{c}(q)}{q^2 \tilde{c}_{\text{hs}}(q)} = \text{constant} - \alpha q. \quad (\text{B5})$$

Hence to determine the exponent α measuring the damping of the hard sphere peaks, we take the ratio of the peak heights of $\tilde{c}(q)$ for the real liquids relative to $\tilde{c}_{\text{hs}}(q)$ from Figure 5.1, $-\alpha$ being the limiting slope as q tends to infinity in a plot of $\ln q^2c(q)/c_{\text{hs}}(q)q^2/q$. In Table II, we record that for

TABLE II

Damping of peaks in experimentally determined structure factors. Form of damping factor employed in quantity $q^2\tilde{c}(q)$ is $\exp(-\alpha q)$.

Liquid	Exponent α in \AA
Pb	0.14
Ar	0.15
Na	> 0.65

Na, $\alpha > 0.65$. This is because a limiting slope was not found within the accessible range of q . No difficulties were found with Pb and Ar; neither is there any doubt, of course, that Na is much the most strongly damped of these three liquids.